

# Sequential Predictive Conformal Inference for Time Series

Chen Xu, Yao Xie\*

H. Milton Stewart School of Industrial and Systems Engineering  
Georgia Institute of Technology

## Abstract

We present a new distribution-free conformal prediction algorithm for sequential data (e.g., time series), called the *sequential predictive conformal inference* (SPCI). We specifically account for the nature that the time series data are non-exchangeable, and thus many existing conformal prediction algorithms based on temporal residuals are not applicable. The main idea is to exploit the temporal dependence of conformity scores; thus, the past conformity scores contain information about future ones. Then we cast the problem of conformal prediction interval as predicting the quantile of a future residual, given a prediction algorithm. Theoretically, we establish asymptotic valid conditional coverage upon extending consistency analyses in quantile regression. Using simulation and real-data experiments, we demonstrate a significant reduction in interval width of SPCI compared to other existing methods under the desired empirical coverage.

## 1 Introduction

Uncertainty quantification for prediction algorithms is essential for statistical and machine learning models. Sequential prediction or time-series prediction aims to predict the subsequent outcome based on past observations. Uncertainty quantification in the form of prediction intervals is of particular interest for high-stake domains such as finance, energy systems, healthcare, and so on [Harries et al., 1999, Díaz-González et al., 2012, Cochran et al., 2015]. Classic approaches for prediction interval are typically based on strong parametric assumptions of time-series models such as autoregressive and moving average (ARMA) models [Brockwell et al., 1991], which impose strong distribution assumptions

---

\*yao.xie@isye.gatech.edu

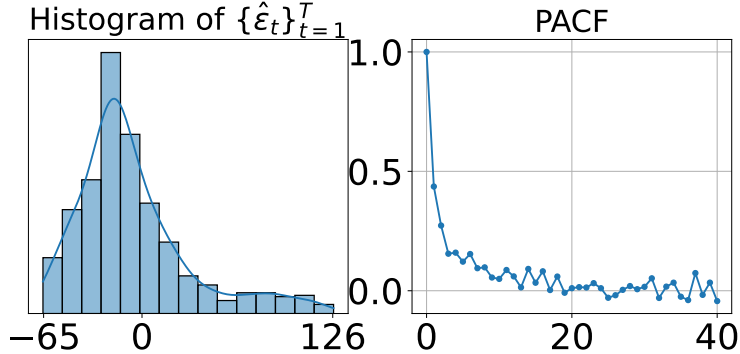


Figure 1: Solar power radiation prediction for downtown Atlanta, Georgia, USA (further explanation in Section 5.3). We use random forest for one-step-ahead prediction. The histogram of prediction residuals (left) shows that residual distribution is highly skewed, and the partial auto-correlation between residuals (right) shows a significant serial correlation among residuals. This example illustrates that it is essential to consider serial dependency when constructing prediction intervals: the serial dependence means that the most recent past residuals contain information about the immediate future ones.

on the data-generating process. There need to be principled ways to perform uncertainty quantification for complex prediction models such as random forests [Breiman, 2001] and neural networks [Lathuilière et al., 2019].

Conformal prediction has become a popular distribution-free technique to perform uncertainty quantification for complex machine learning algorithms. However, conformal prediction for time series has been a challenging case because they do not satisfy the exchangeability assumption typically assumed in conformal inference, and thus we need to adjust existing or even develop new algorithms with theoretical guarantees. The challenges also arise in real-world applications where time series data tend to have significant stochastic variations and strong correlations. These challenges are illustrated via a real-data example for solar energy prediction, as shown in Figure 1, where the residuals are still highly correlated after applying a sequential random forest predictor. Besides the serial correlation in the prediction residuals (or conformity scores in general), we observe that a notable feature of sequential conformal prediction is that the prediction residuals can be obtained as “feedback” to the algorithm. For instance, for one-step ahead prediction, the prediction accuracy of the prediction algorithm is revealed immediately after one-time step. Thus, the recent prediction residuals reveal whether or not the predictive algorithm is performing well for that segment of data. Such feedback structure is illustrated in Figure 2, which highlights the conceptual difference between traditional conformal and sequential conformal prediction methods. We specifically exploited such feedback structure in designing the sequential conformal prediction algorithms.

In this work, we propose a *sequential predictive conformal inference* (SPCI) framework for time series with scalar outputs. The idea is to utilize the feedback structure of prediction

residuals in the sequential prediction problem to obtain good instantaneous coverage. We specifically exploit the serial dependence across prediction residuals (conformity score); thus, the most recent past residuals contain information about the immediate future ones by performing quantile regression using past residuals for the future prediction intervals. Similar to most existing conformal prediction literature, we make no assumptions about the data-generating process or the quality of estimation by the point estimator. We can show the asymptotic conditional coverage of the constructed intervals when data are dependent based on prior results for random forest quantile regression. Moreover, when data are further exchangeable, we show that **SPCI** enjoys the same finite-sample and distribution-free marginal coverage guarantee as traditional conformal prediction methods. Experimentally, we demonstrate the improved performance by **SPCI** over existing conformal prediction methods on real-world time-series data: **SPCI** achieves narrower interval width under the same valid interval coverage than state-of-the-art methods. We further demonstrate the applicability and benefit of **SPCI** for constructing multiple prediction intervals simultaneously beyond one-step-ahead prediction.

## 1.1 Literature review

Conformal prediction (CP) has been an increasingly popular framework for distribution-free uncertainty quantification. Initially proposed in [Shafer and Vovk, 2008], CP methods generally proceed as follows. First, one designs a type of “non-conformity score” based on the given point estimator  $\hat{f}$ , where the score measures how different a potential value of the response variable  $Y$  is to existing observations. A common choice for such scores in regression problems is the prediction residual. Second, one computes these scores on a *hold-out* set not used to train the estimator  $\hat{f}$ . Third, the prediction interval is defined as all potential values of  $Y$  whose non-conformity score is less than  $1 - \alpha$  fraction of these scores over the hold-out set. Many existing works such as [Papadopoulos et al., 2007, Gupta et al., 2021, Angelopoulos et al., 2021, Romano et al., 2020] utilize this idea for uncertainty quantification in regression or classification problems. Comprehensive surveys and tutorials can be found in [Zeni et al., 2020, Angelopoulos and Bates, 2021]. CP framework are distribution-free and model-free: they require neither distributional assumptions on data nor special classes of prediction functions, hence being particularly attractive in practice. Nevertheless, the desired performance guarantee of CP methods relies on *exchangeability* (e.g., the simplest case is when data are i.i.d.), which hardly holds for time series.

Compared the traditional conformal inference and the sequential conformal inference considered in this paper, both are general-purpose wrappers that can be used around any predictive model for any data and proceed by defining “non-conformity scores” (e.g., prediction residual  $\hat{\epsilon}_t := Y_t - \hat{Y}_t$ ). However, there are also significant differences: Traditional conformal prediction assumes exchangeable training and test data to obtain performance guarantees, which leads to exchangeable non-conformity scores, and cannot receive feedback during prediction. In contrast, sequential CP observes non-exchangeable data sequences

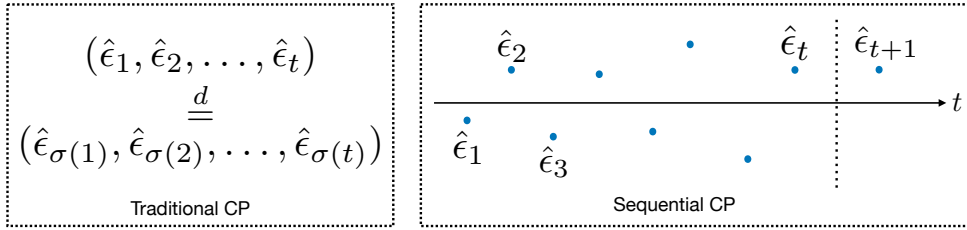


Figure 2: Differences between traditional and sequential Conformal Prediction (CP) methods. In traditional CP, residuals are exchangeable, and the same set of residuals is used throughout the prediction. In contrast, sequential CP assumes an ordering of the potentially non-exchangeable residuals; residuals are available feedback to the prediction algorithms: past residuals are updated to include the new prediction residual  $\hat{\epsilon}_{t+1}$  during prediction.

and leverages feedback during prediction.

Recently, significant efforts have been made to extend CP methods beyond exchangeable data; several are towards building sequential conformal prediction methods. They typically do so via updating non-conformity scores (e.g., prediction residuals) [Xu and Xie, 2021] and/or adjust significance level  $\alpha$  based on rolling coverage of  $Y_t$ . This include [Gibbs and Candes, 2021, Zaffran et al., 2022] and AdaptCI algorithm, which adjusts the significance level  $\alpha$  based on real-time coverage status during prediction—the significance level is lower when the prediction interval at time  $t$  fails to contain the actual observation  $Y_t$ . The prediction intervals thus have adaptive width based on the updated significance levels and maintain coverage on stock market data in practice. Furthermore, Barber et al. [2022] proves the coverage gap for non-exchangeable data based on the total variation (TV) distance between the non-conformity scores. The work then proposes NEX-CP, a general re-weighting scheme for non-exchangeable data, where the weights should ideally be chosen to be inversely proportional to the TV distances. The authors demonstrate the robustness of NEX-CP on datasets with change points and/or distribution shifts. For sequential data, Xu and Xie [2021] proposes EnbPI, which updates residuals of ensemble predictors during prediction to more accurately calibrate prediction intervals. In practice, EnbPI can maintain desired  $1 - \alpha$  coverage even for non-stationary time series. Despite the existing efforts, these sequential CP methods have not exploited serial correlation among non-conformity scores (cf. Figure 1)—they only use empirical quantiles (possibly with fixed weights) of past non-conformity scores to compute prediction intervals, which is a drastic difference from SPCI.

We further remark on several key differences of SPCI with prior works. Method-wise, our prediction intervals are constructed using conditional quantile regression functions on *non-conformity scores* (e.g., residuals). In contrast, existing quantile-regression-based methods [Romano et al., 2019, Gupta et al., 2021] directly fits conditional quantile functions on the response variables  $Y$ , after which the intervals are constructed using *empirical quantiles* of non-conformity scores, and thus our approach can further leveraging existing

strong prediction algorithm to handle data non-stationarity. Theory-wise, we obtain similar asymptotic conditional coverage for dependent residuals as in [Xu and Xie, 2021]. However, different from that work, we do not assume a particular functional form of the conditional distribution of the scalar output given feature variables.

## 2 Problem setup

Assume a sequence of observations  $(X_t, Y_t)$ ,  $t = 1, 2, \dots$ , where  $Y_t$  are continuous scalar variables and  $X_t \in \mathbb{R}^d$  denote features, which may either be the history of  $Y_t$  or contain exogenous time-series helpful in predicting the value of  $Y_t$ . We can allow observations to be highly correlated under an unknown conditional distribution  $Y_t|X_t, \dots, X_1$ , and do not assume a particular functional form of the conditional distribution  $Y_t|X_t, \dots, X_1$ . Let the first  $T$  samples  $\{(X_t, Y_t)\}_{t=1}^T$  be the training data.

Our goal is to construct prediction intervals sequentially starting from time  $T + 1$  such that the prediction intervals will contain the true outcome with a pre-specified high probability  $1 - \alpha$  while the prediction interval is as narrow as possible. Here the *significance level*  $\alpha$  is user-specified. The prediction intervals  $\hat{C}_{t-1}(X_t)$ , which depend on  $\alpha$ , are around point predictions  $\hat{Y}_t := \hat{f}(X_t)$  for a given predictive model  $\hat{f}$ . We emphasize that our algorithm provides prediction intervals for an arbitrary user-chosen predictive algorithm. Here the subscript  $t-1$  indicates the interval is constructed using previous up to  $t - 1$  many observations.

There are two types of coverage guarantees to be satisfied by  $\hat{C}_{t-1}(X_t)$ . The first is the weaker *marginal* coverage:

$$\mathbb{P}(Y_t \in \hat{C}_{t-1}(X_t)) \geq 1 - \alpha, \forall t, \quad (1)$$

while the second is the stronger *conditional* coverage:

$$\mathbb{P}(Y_t \in \hat{C}_{t-1}(X_t)|X_t) \geq 1 - \alpha, \forall t. \quad (2)$$

If  $\hat{C}_{t-1}(X_t)$  satisfies (1) or (2), it is called marginally or conditionally valid, respectively. In terms of the interval width, to avoid vacuous prediction interval  $\hat{C}_{t-1}(X_t)$  (in the extreme case, if one chooses the entire real line for all  $t$ , it will always contain the true outcome  $Y_t$  with high probability), we should construct intervals with width  $|\hat{C}_{t-1}(X_t)|$  as narrow as possible.

A natural approach in developing sequential CP methods is constructing sequential prediction intervals using the most recent feedback in predicting  $Y_t$ , as shown in Figure 3. However, only considering the empirical distribution of residuals may not fully exploit the temporal dependence across the residuals. Indeed, when residuals are temporally correlated, the past residuals contain information about the distribution of future residuals and can be used to perform “predictive” conformal inference. More precisely, we should use the past residuals to predict the tail probability of the new residual, which may allow certain adaptivity. The above is the main idea of our proposed SPCI algorithm.

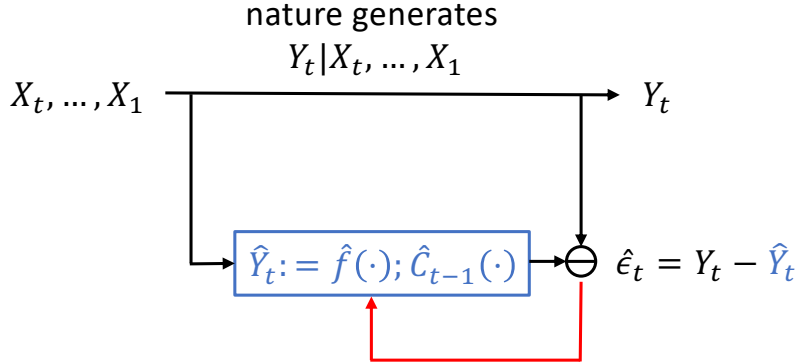


Figure 3: Unlike traditional CP methods, sequential CP methods leverage feedback (in red arrow) during prediction. Here we use prediction residual  $\hat{\epsilon}_t := Y_t - \hat{Y}_t$  as an example of the non-conformity score.

### 3 Algorithms

Below, we first consider a simple split conformal prediction as a vanilla baseline approach based on traditional CP, which constructs prediction intervals without considering feedback during prediction. Then, we present the `EnbPI` [Xu and Xie, 2021] method in sequential CP as a refined approach and illustrate its limitation in using empirical quantile of past residuals. Then we introduce the proposed `SPCI` as an improved algorithm for sequential CP for time series data.

#### 3.1 Vanilla split conformal

One of the most commonly used conformal prediction methods is *split conformal*, so we use it as a prototypical example [Papadopoulos et al., 2007]. First, split the indices of training data  $[T] := \{1, \dots, T\}$  into two halves  $\mathcal{I}_1$  and  $\mathcal{I}_2$ . Second, fit the prediction model  $\hat{f}$  on  $\{(X_t, Y_t), t \in \mathcal{I}_1\}$  to make point predictions  $\hat{Y}_t := \hat{f}(X_t), t \notin \mathcal{I}_1$ . Third, compute *non-conformity score* on  $\mathcal{I}_2$ . A typical choice is a prediction residual  $\hat{\epsilon}_t := Y_t - \hat{Y}_t$ . Lastly, define the prediction interval for  $t > T$  as

$$\hat{C}_{t-1}(X_t) := [\hat{f}(X_t) + q_{\alpha/2}(\{\hat{\epsilon}_j\}_{j \in \mathcal{I}_2}), \hat{f}(X_t) + q_{1-\alpha/2}(\{\hat{\epsilon}_j\}_{j \in \mathcal{I}_2})], \quad (\text{Split conformal}) \quad (3)$$

where  $q_{1-\alpha}$  is the  $1 - \alpha$  quantile function over a set of values. In particular, the set of non-conformity scores  $\{\hat{\epsilon}_j\}_{j \in \mathcal{I}_2}$  is fixed during prediction. When  $(X_t, Y_t)$  are exchangeable (i.e., we can shuffle the order of these random variables without affecting the joint distribution), split conformal intervals in (3) reaches exact finite-sample marginal coverage defined in (2). However, without further distribution assumptions, split conformal intervals cannot reach valid conditional coverage in (2) [Foygel Barber et al., 2021].

### 3.2 EnbPI: An ensemble version using empirical residuals

Compared to split conformal in the previous section, EnbPI involves no data-splitting, trains ensemble predictors that make more accurate point predictions and utilizes feedback during prediction on test data. Thus, EnbPI is more suitable than split conformal for sequential prediction interval construction. EnbPI has the following three steps. First, it leverages training data as much as possible by fitting “leave-one-out” (LOO) ensemble prediction models  $\hat{f}_t(X_t) := \phi(\{\hat{f}_b(X_t) : t \notin S_b\})$ , where  $S_b \subset [T]$  is the bootstrap index set used to train the  $b$ -th bootstrap estimator  $\hat{f}_b$ . The point predictor on test data is defined as  $\hat{f}(X_t) := \phi(\{\hat{f}_b(X_t)\})$ , which aggregates all bootstrap predictions. Second, we obtain residuals using the LOO models  $\hat{\epsilon}_t := Y_t - \hat{f}_t(X_t)$ . Third, it updates the past residuals during predictions so that the prediction intervals have adaptive width. For a fixed  $w \geq 1$ , denote  $\mathcal{E}_t^{-w} := \{\hat{\epsilon}_{t-1}, \dots, \hat{\epsilon}_{t-w}\}$  as the past  $w$  residuals. Then, EnbPI intervals have the form:

$$\hat{C}_{t-1}(X_t) := [\hat{f}(X_t) + q_{\alpha/2}(\mathcal{E}_t^{-T}), \hat{f}(X_t) + q_{1-\alpha/2}(\mathcal{E}_t^{-T})], \quad (\text{EnbPI}) \quad (4)$$

which greatly resemble traditional CP intervals in (3) due to the use of empirical quantile function  $q_{1-\alpha}$  to compute interval width.

However, EnbPI intervals in (4) can have limitations under dependent residuals. Note that dependent residuals lead to non-equivalence between conditional and marginal distributions of  $\hat{\epsilon}_t$ , namely:

$$\hat{\epsilon}_t | \mathcal{E}_t^{-w} \stackrel{d}{\neq} \hat{\epsilon}_t. \quad (5)$$

Let  $F(z | \mathcal{E}_t^{-w}) := \mathbb{P}(\hat{\epsilon}_t \leq z | \mathcal{E}_t^{-w})$  be the unknown conditional distribution function of the residual  $\hat{\epsilon}_t$ . Based on (4),

$$\begin{aligned} \mathbb{P}(Y_t \in \hat{C}_{t-1}(X_t) | X_t) &= \mathbb{P}(\hat{\epsilon}_t \in [q_{\alpha/2}(\mathcal{E}_t^{-T}), q_{1-\alpha/2}(\mathcal{E}_t^{-T})] | X_t) \\ &= F(q_{1-\alpha/2}(\mathcal{E}_t^T) | \mathcal{E}_t^w) - F(q_{\alpha/2}(\mathcal{E}_t^T) | \mathcal{E}_t^w). \end{aligned} \quad (6)$$

However, the distribution function  $F$  evaluated at the empirical quantiles may not yield the desired coverage. More precisely, define

$$Q_t(p) := \inf\{e^* \in \mathbb{R} : F(e^* | \mathcal{E}_t^{-w}) \geq p\}, \quad (7)$$

which is the  $p$ -th quantile of the residual  $\hat{\epsilon}_t$ . By definition,

$$F(Q_t(1 - \alpha/2) | \mathcal{E}_t^w) - F(Q_t(\alpha/2) | \mathcal{E}_t^w) = 1 - \alpha. \quad (8)$$

Thus, in order for EnbPI intervals in (4) to have the desired  $1 - \alpha$  coverage asymptotically, the empirical quantile must uniformly converge to the actual quantile value, namely:

$$\sup_{p \in [0,1]} |q_p(\mathcal{E}_t^{-T}) - Q_t(p)| \rightarrow 0 \text{ as } T \rightarrow \infty. \quad (9)$$

However, the condition (9) requires strong assumptions: [Xu and Xie, 2021] assumes a particular linear functional form of  $Y_t | X_t$  (i.e.,  $Y_t = f(X_t) + \epsilon_t$ ), which further needs to be consistently estimated as sample size approaches infinity. Such assumptions can impose limitations in practice.

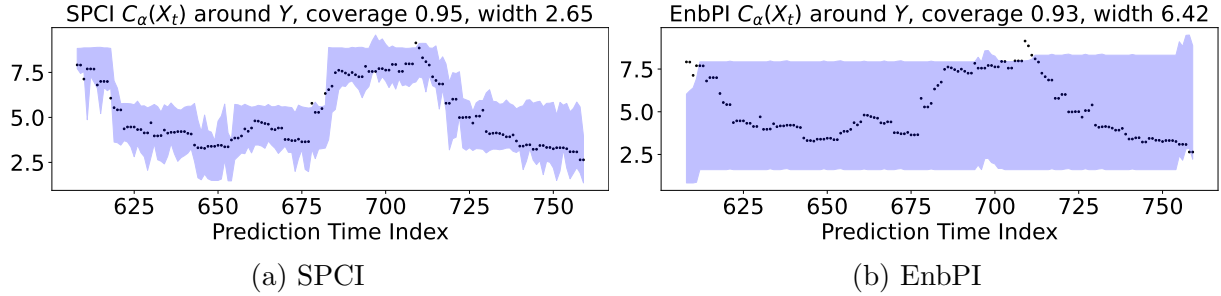


Figure 4: SPCI advantage over EnbPI: both have the same coverage but SPCI yields significantly narrower intervals due to the use of conditional quantile estimators of residuals.

### 3.3 Proposed SPCI algorithm

Due to the limitations above by split conformal and EnbPI, we propose SPCI as a more general framework than both approaches. In particular, EnbPI directly leverages the dependency of  $\hat{\epsilon}_t$  on the past residuals when constructing the prediction intervals. Based on the equivalence in (6) and the exact coverage property in (8), SPCI replaces the empirical quantile with an estimate by a conditional quantile estimator. Specifically, let  $\hat{Q}_t(p)$  be an estimator of the true quantile  $Q_t(p)$  in (7). Then, SPCI intervals are defined as

$$\hat{C}_{t-1}(X_t) := [\hat{f}(X_t) + \hat{Q}_t(\alpha/2), \hat{f}(X_t) + \hat{Q}_t(1 - \alpha/2)], \quad (\text{SPCI}) \quad (10)$$

where the point predictor  $\hat{f}$  is a pre-trained model. In particular, if we train LOO point predictors and choose the quantile estimator  $\hat{Q}_t(\cdot)$  as the empirical quantile, SPCI in (10) reduces to EnbPI in (4). Furthermore, if we follow split conformal prediction to train the point predictor and do no update residuals during predictions, SPCI intervals also reduce to the split conformal intervals in (3).

Algorithm 1 presents the details of SPCI, whose main novelty lies in using an estimated quantile function instead of the empirical quantile function. We intentionally simplify the descriptions of how to train the point estimator  $\hat{f}$  and compute prediction residuals to allow for greater flexibility. One can either adopt a split conformal strategy as in (3) or use the LOO fitting as in EnbPI (4). The former is more computationally efficient but tends to suffer from less accurate point predictions and, therefore, wider intervals.

We particularly comment on the computational aspect of fitting conditional quantile regression algorithm for Algorithm 1, which is the essential step of SPCI. Note that fitting quantile regressors require minimization of the following pinball loss

$$\mathcal{L}(x, \alpha) = \begin{cases} \alpha x & \text{if } x \geq 0, \\ (\alpha - 1)x & \text{if } x < 0, \end{cases} \quad (11)$$

which depends on the significance level  $\alpha$ . Because SPCI aims to produce intervals as narrow as possible (see line 3) and refits the quantile regression models under need feedback

---

**Algorithm 1** Sequential Predictive Conformal Inference (SPCI)

---

**Require:** Training data  $\{(X_t, Y_t)\}_{t=1}^T$ , significance level  $\alpha$ , conditional quantile regression algorithm  $\mathcal{Q}$ .

**Ensure:** Prediction intervals  $\hat{C}_{t-1}(X_t), t > T$

- 1: Train a point estimator  $\hat{f}$  and obtain the list of *prediction* residuals  $\hat{\epsilon}$ .
- 2: **for**  $t > T$  **do**
- 3:   Compute  $\hat{\beta} = \arg \min_{\beta \in [0, \alpha]} (\hat{Q}_t(1 - \alpha + \beta) - \hat{Q}_t(\beta))$ , where  $\{\triangleright$  Minimize width. $\}$   
       $\hat{Q}_t := \mathcal{Q}(\hat{\epsilon})$  is the fitted quantile regressor.
- 4:    $\hat{C}_{t-1}(X_t) = [\hat{Y}_t + w_{\text{left}}(t), \hat{Y}_t + w_{\text{right}}(t)]$ , where  
       $\hat{Y}_t = \hat{f}(X_t)$ ,  $w_{\text{left}}(t) = \hat{Q}_t(\hat{\beta})$ ,  $w_{\text{right}}(t) = \hat{Q}_t(1 - \alpha + \hat{\beta})$
- 5:   **if**  $Y_t$  is observed as feedback **then**
- 6:      $\hat{\epsilon}.\text{pop}(1)$  and  $\hat{\epsilon}.\text{append}(Y_t - \hat{Y}_t)$ .  $\{\triangleright$  Update residual. $\}$
- 7:     Re-fit  $\hat{Q}_t = \mathcal{Q}(\hat{\epsilon})$
- 8:   **end if**
- 9: **end for**

---

(see line 7), it is important to choose quantile regression algorithms that are efficient enough in this sequential setting. In this work, we will use quantile random forest (QRF) [Meinshausen, 2006] as the quantile regression estimator and establish the corresponding coverage guarantees.

## 4 Theory

We first show that when data are exchangeable, one can reach exact marginal coverage when using the empirical quantile function as the quantile regression predictor. We then establish asymptotic coverage upon considering the dependency of estimated residuals. Most proofs and additional theoretical details appear in Appendix A.

### 4.1 Under exchangeability

Although SPCI is designed for time-series predictive inference, we show that simple modifications of SPCI as shown in Algorithm 2 reduce SPCI to the split conformal prediction method [Papadopoulos et al., 2007], whose interval construction was described in (3). In particular, the modifications are (a) train point predictors via data-splitting, (b) use empirical quantile functions as the conditional quantile estimator, and (c) do not update test residuals in prediction. Because split conformal prediction yields finite-sample marginal coverage for exchangeable observations, so does SPCI.

**Proposition 1** (Finite-sample marginal coverage under exchangeability [Papadopoulos et al., 2007]). *Suppose the data  $(X_t, Y_t), t \geq 1$  are exchangeable (e.g., independent and*

---

**Algorithm 2** SPCI for exchangeable data (based on split conformal)

---

**Require:** Training data  $\{(X_t, Y_t)\}_{t=1}^T$ , significance level  $\alpha$ .

**Ensure:** Prediction intervals  $\hat{C}_{t-1}(X_t), t > T$

- 1: Randomly split  $\{1, \dots, T\}$  into disjoint index sets  $\mathcal{I}_1$  and  $\mathcal{I}_2$ .
- 2: Train a point predictor  $\hat{f}$  with  $\{(X_t, Y_t)\}_{t \in \mathcal{I}_1}$ .
- 3: Obtain residuals  $\hat{\epsilon}_t := Y_t - \hat{f}(X_t)$  for  $t \in \mathcal{I}_2$ .
- 4: **for**  $t > T$  **do**
- 5:     Return the prediction interval  $\hat{C}_{t-1}(X_t)$  as in (3).
- 6: **end for**

---

*identically distributed). Prediction intervals obtained via Algorithm 2 satisfy*

$$\mathbb{P}(Y_t \in \hat{C}_{t-1}(X_t)) \geq 1 - \alpha.$$

*Proof.* The proof is standard in conformal prediction literature based on an exchangeability argument. By (3), we know that

$$\mathbb{P}(Y_t \in \hat{C}_{t-1}(X_t)) = \mathbb{P}(\hat{\epsilon}_t \in [q_{\alpha/2}(\{\hat{\epsilon}_j\}_{j \in \mathcal{I}_2}), q_{1-\alpha/2}(\{\hat{\epsilon}_j\}_{j \in \mathcal{I}_2})]).$$

By exchangeability of the original data and the fact that  $\hat{f}$  is trained on  $(X_t, Y_t), t \in \mathcal{I}_1$ , we have  $\{\hat{\epsilon}_j\}_{j \in \mathcal{I}_2}$  and  $\hat{\epsilon}_t$  are exchangeable. For  $p \in [0, 1]$ , let  $q_p := q_{\alpha/2}(\{\hat{\epsilon}_j\}_{j \in \mathcal{I}_2})$ . Thus, by property of exchangeability, we have

$$\begin{aligned} \mathbb{P}(\hat{\epsilon}_t \in [q_{\alpha/2}, q_{1-\alpha/2}]) &= \frac{1}{|\mathcal{I}_2|} \sum_{j \in \mathcal{I}_2} \mathbb{P}(\hat{\epsilon}_j \in [q_{\alpha/2}, q_{1-\alpha/2}]) \\ &= \frac{1}{|\mathcal{I}_2|} \mathbb{E} \left[ \sum_{j \in \mathcal{I}_2} \mathbb{1}(\hat{\epsilon}_j \in [q_{\alpha/2}, q_{1-\alpha/2}]) \right] = 1 - \alpha, \end{aligned}$$

where the last equality holds by the definition of the interval  $[q_{\alpha/2}, q_{1-\alpha/2}]$ .  $\square$

## 4.2 Beyond exchangeability

The primary theoretical contribution of our work is to show the asymptotic conditional validity of SPCI intervals when the quantile random forest [Meinshausen, 2006] is used as the conditional quantile estimator. Specifically, we show that

$$\mathbb{P}(Y_t \in \hat{C}_{t-1}(X_t) | X_t) \rightarrow 0 \text{ as } T \rightarrow \infty,$$

which by (6) and (7), is equivalent to proving

$$\sup_{p \in [0, 1]} |\hat{Q}_t(p) - Q_t(p)| \rightarrow 0 \text{ as } T \rightarrow \infty, \quad (12)$$

where  $\widehat{Q}_t(p)$  is the QRF estimator. Note that (12) for i.i.d. observations has been proven in [Meinshausen, 2006, Theorem 1], so that our analysis also extends the original statement therein to observations with dependency.

We follow the notation in [Meinshausen, 2006] to introduce QRF. For every feature  $X_t, t \geq 1$ , assume its support  $\text{Supp}(X_t) \subset \mathbb{B} \subset \mathbb{R}^d$ . We grow the tree  $T(\theta)$  with parameter  $\theta$  as follows: every leaf  $l = 1, \dots, L$  of a tree  $T(\theta)$  is associated with a rectangular subspace  $R_l \subset \mathbb{B}$ . In particular, they are disjoint and cover the entire space  $\mathbb{B}$ : for every  $x \in \mathbb{B}$ , there is *one and only one* leaf  $l$ , thus denoted as  $l(x, \theta)$ , such that  $x \in R_{l(x, \theta)}$ . If we grow  $K$  trees, let each of them have separate parameter  $\theta_k$ . Now, for a given  $x \in \mathbb{B}$  and  $T$  observed features  $X_1, \dots, X_T$ , we define the following weights:

$$k_\theta(l) := \#\{j \in \{1, \dots, n\} : X_j \in R_{l(x, \theta)}\} \quad (13)$$

$$w_t(x, \theta) := \frac{\mathbb{1}(X_t \in R_{l(x, \theta)})}{k_\theta(l)} \quad (14)$$

$$w_t(x) := K^{-1} \sum_{k=1}^K w_t(x, \theta_k) \quad (15)$$

For interpretation, (13) counts the “node size” of the leave  $l(x, \theta)$ , (14) weighs the  $i$ -th observation using whether  $X_t$  belongs to this leave and its node size, and (15) weighs such weights from  $K$  trees. Note that by definition, we must have  $\sum_{t=1}^T w_t(x) = 1$ . Finally, based on weights in (15), the estimated conditional distribution function  $\hat{F}(y|x)$  by QRF on  $T$  samples  $\{(X_t, Y_t)\}_{t=1}^T$  is defined as

$$\hat{F}(y|x) := \sum_{t=1}^T w_t(x) \mathbb{1}(Y_t \leq y). \quad (16)$$

In retrospect, the empirical distribution in (16) is similar to that under fixed weights by [Barber et al., 2022]. The key difference is that (16) uses data-adaptive weights whereas [Barber et al., 2022] uses fixed and non-adaptive weights.

To show the convergence of the estimated QRF quantile to the true value, we first have the following lemma relating the convergence of quantile estimates to the convergence of corresponding distribution functions.

**Lemma 1.** *For random variable  $Y$ , let  $F(y|x)$  be its conditional distribution function and  $Q(p) := \inf\{y \in \mathbb{R} : F(y|x) \geq p\}$  be the  $p$ -th quantile, which is assumed to be unique. Let  $\hat{F}(y|x)$  be an estimator trained on  $T$  samples  $\{(X_t, Y_t)\}_{t=1}^T$ . If for all  $y$  and  $x$  it holds that*

$$\hat{F}(y|x) \rightarrow F(y|x) \text{ in probability,} \quad (17)$$

*then  $\widehat{Q}(p) := \inf\{y \in \mathbb{R} : \hat{F}(y|x) \geq p\}$  satisfies  $\widehat{Q}(p) \rightarrow Q(p)$  in probability for every  $p \in (0, 1)$  and  $x$ .*

Thus, the crux of the remaining analyses relies on showing the point-wise convergence in (17) for the QRF in (16). The case where all data are independent and identically distributed has been addressed in [Meinshausen, 2006, Theorem 1]. We address the more general case in Proposition 2.

**Proposition 2.** *If Assumptions 1–4 defined in Appendix A hold, we obtain the point-wise convergence in (17) for QRF.*

**Theorem 1** (Asymptotic conditional coverage beyond exchangeability). *Let QRF be the conditional quantile algorithm  $\mathcal{Q}$  used in Algorithm 1, line 9. Under the same assumptions as Lemma 1 and Proposition 2, as the sample size  $T \rightarrow \infty$ , we have for any  $\alpha \in (0, 1)$*

$$|\mathbb{P}(Y_t \in \hat{C}_{t-1}(X_t) | X_t) - (1 - \alpha)| \rightarrow 0 \text{ in probability.} \quad (18)$$

**Remark 1** (Interval convergence). *Ideally, we wish SPCI intervals in (10) to converge in width to the oracle interval defined by  $Y_t | X_t$ . However, doing so requires assumptions on the inverse CDF of  $Y_t | X_t$ , which deviate from our focus on model-free interval construction. Even though such theoretical analyses are lacking, experiments in Section 5 demonstrate that SPCI improves over recent sequential conformal prediction models in many cases.*

**Remark 2** (Generality of QRF). *Note that decision trees are simple functions, thus satisfying the assumptions of the Simple Function Approximation Theorem [Royden and Fitzpatrick, 1988]. In other words, the QRF estimates can theoretically approximate those of any other quantile estimates. As a result, this can be useful if one analyzes the convergence of QRF quantile estimates for residuals with a more general dependency.*

**Remark 3** (Convergence beyond using QRF). *The convergence of quantile estimates has been a long-standing question in statistics. In our case, we are particularly interested in the quantile estimates under time-series data. In the past, several lines of work have established such results for different estimators under various assumptions on dependency. [Cai, 2002] studied weighted Nadaraya-Watson quantile estimates for  $\alpha$ -mixing sequences. [Biau and Patra, 2011] proposes a nearest-neighbor strategy for stationary and ergodic data. [Zhou and Wu, 2009] analyzed local linear quantile estimators for locally stationary time series. More analyses appear in the survey [Xiao, 2012].*

## 5 Experiments

We empirically demonstrate the improved performance of SPCI over competing sequential CP methods on simulated and real data in terms of interval coverage and width.

### 5.1 Baseline methods

We compare SPCI with three recently introduced CP methods for non-exchangeable data or time series, which have also been mentioned in the literature review. In particular, they all leverage the feedback  $Y_t$  after it is sequentially revealed.

- EnbPI [Xu and Xie, 2021] proposes a general framework for constructing time-series prediction intervals. In particular, it is identical to SPCI in terms of the procedure for fitting LOO regression models and using residuals as non-conformity scores. Thus, the only difference appears in conditional rather than empirical quantiles for width calibration.
- AdaptiveCI [Gibbs and Candes, 2021] is an adaptive procedure that adjusts the significance level  $\alpha$  based on historical information of interval coverage. It leverages CQR [Romano et al., 2019] to produce intervals that maintain coverage validity and have a narrower width than competing methods on non-exchangeable data. We use the quantile random forest as the predictor and update  $\alpha$  according to the simple online update (ibid., Eq (2)).
- NEX-CP [Barber et al., 2022] uses weighted quantiles to tackle arbitrary distribution drift in test data. In particular, the implementation is based on full conformal with weighted least squares regression models, which empirically yields more stable coverage than the naive split conformal method.

## 5.2 Simulated data results

We compare SPCI with EnbPI on non-stationary and/or heteroskedastic time-series. Given a feature  $X_t$ , we specify the true data-generating process as

$$Y_t = f(X_t) + \epsilon_t. \quad (19)$$

We simulate two types of time-series data based on (19):

1. Non-stationary time-series: We let

$$\begin{aligned} f(X_t) &= g(t)h(X_t). \\ g(t) &= \log(t') \sin(2\pi t'/12), t' = \text{mod}(t, 12). \\ h(X_t) &= (|\beta^T X_t| + (\beta^T X_t)^2 + |\beta^T X_t|^3)^{1/4}. \end{aligned} \quad (20)$$

Note that the model in (20) can represent non-stationary time-series due to additional time-related effects (e.g., time drift, seasonality, periodicity, etc.). For a fixed window size  $w \geq 1$ , each feature observation  $X_t = Y_t^{-w} := [Y_{t-w}, \dots, Y_{t-1}]$  contains the past  $w$  observations of the response  $Y$ . We sample the errors  $\epsilon_t$  from an AR(1) process, where  $\epsilon_t = \rho\epsilon_{t-1} + e_t$  and  $e_t$  are *i.i.d.* normal random variables with zero mean and unit variance with  $\rho = 0.6$ . Because  $f$  in (20) explicitly depend on  $t$  and  $X_t$ , we use the new feature  $\tilde{X}_t := [\text{mod}(t, 12), X_t]$  to predict  $Y_t$ .

2. Heteroskedastic time-series: We let

$$f(X_t) = (|\beta^T X_t| + (\beta^T X_t)^2 + |\beta^T X_t|^3)^{1/4}. \quad (21)$$

$$\text{Var}(\epsilon_t) = \sigma(X_t)^2, \sigma(X_t) = \mathbf{1}^T X_t. \quad (22)$$

Table 1: Simulation: **EnbPI** vs. **SPCI** on simulated time-series with  $\alpha = 0.1$ . **SPCI** outperforms **EnbPI** in terms of interval width without sacrificing valid coverage.

	Non-stationary coverage	Non-stationary width	Heteroskedastic coverage	Heteroskedastic width
SPCI	0.94 (2.04e-03)	11.23 (3.37e-02)	0.89 (9.43e-03)	24.09 (8.27e-01)
EnbPI	0.91 (1.11e-16)	25.22 (2.84e-02)	0.92 (1.18e-02)	25.84 (3.47e-01)

Note that the model above represents the generalized autoregressive conditional heteroskedasticity (GARCH) model [Engle, 1982], where variances of response  $Y_t$  depend on its feature  $X_t$ . We let features  $X_t \in \mathbb{R}^{20}$ , with i.i.d. entries from  $\text{Uniform}[0, e^{0.01\text{mod}(t, 100)}]$ . Due to heteroskedastic errors, we estimate conditional quantile of normalized residuals  $\hat{\epsilon}_t := (Y_t - \hat{f}_t(X_t))/\hat{\sigma}(X_t)$  and multiply the quantile values by estimates  $\hat{\sigma}(X_t)$  to construct the prediction intervals.

Table 1 compares **EnbPI** with **SPCI**, where **SPCI** shows clear improvement. We suspect the improvement lies in the more adaptive and accurate calibration of quantile values of residual distributions in prediction.

### 5.3 Real-data results

Unless otherwise specified, we fix  $\alpha = 0.1$  and use the first 80% (resp. rest 20%) data for training (resp. testing). For **SPCI** and **EnbPI**, we use the random forest regression model with 25 bootstrap models.

*Datasets.* Three real time series are used. The first dataset is the wind speed data (m/s) at wind farms operated by the Midcontinent Independent System Operator (MISO) in the US [Zhu et al., 2021]. The wind speed record was updated every 15 minutes over a one-week period in September 2020. The second dataset contains solar radiation information<sup>1</sup> in Atlanta downtown, which is measured in Diffuse Horizontal Irradiance (DHI). The full dataset contains a yearly record in 2018 and is updated every 30 minutes. We remark that uncertainty quantification for both wind and solar is important for accurate and reliable energy dispatch. The last dataset tracks electricity usage and pricing [Harries et al., 1999] in the states of New South Wales and Victoria in Australia, with an update frequency of 30 minutes over a 2.5-year period in 1996–1999. We are interested in tracking the quantity of electricity transferred between the two states.

*Marginal results.* Table 2 shows the marginal coverage and width of all four methods on the three time series. While all methods nearly maintain validity at  $\alpha = 0.1$ , **SPCI** yields significantly narrower intervals, especially on the wind speed prediction data. Such results illustrate the advantages of fitting conditional quantile regression on residuals for width calibration and training LOO regression predictors for point prediction.

<sup>1</sup>Collected from National Solar Radiation Database (NSRDB): <https://nsrdb.nrel.gov/>.

*Rolling results.* Besides the marginal metric, we hereby provide further insights into the dynamics of prediction intervals. Figure 5 visualizes the rolling coverage and width of each method, where the metric is computed over a rolling window of size 100 (resp. 50) for the solar and electricity (resp. wind) datasets. The results show that (1) **SPCI** barely loses rolling coverage when competing methods (e.g., **EnbPI**) can fail to do so. (2) **SPCI** intervals are adaptive: they are wider or narrower depending on the data index, which likely reflects higher or less uncertainty in test data. (3) **SPCI** intervals are evidently narrower than those by competing methods. (4) **SPCI** rolling results have less variance than others such as **NEX-CP**.

## 6 Multi-step prediction

In practice, constructing multiple prediction intervals at once is essential. Thus, we modify **SPCI** in Algorithm 1 to examine its performance on the more challenging multi-step prediction task.

*Motivation and setup.* We first motivate the study of multi-step ahead prediction interval. In previous examples, all intervals are one step ahead: the response variable  $Y_t$  is revealed *before*  $C_{t+1}(\alpha)$  is constructed, which is the prediction interval for  $Y_{t+1}$ . Such immediate feedback is advantageous for all adaptive methods as they thus have access to the most up-to-date information about the data process. Nevertheless, such access can be neither feasible nor desirable for some use cases. In energy systems such as wind or solar prediction, we often need multiple forecasts spanning a long enough future horizon to allow enough time for subsequent dispatch. Meanwhile, lags in data collection can limit the availability of feedback—for  $S > 1$ ,  $Y_t$  may not be revealed until the  $S$ –step ahead interval  $C_{t+S}(\alpha)$  is constructed.

We consider the following multi-step ahead prediction setting. Fix a value of  $S \geq 1$ , which denotes the  $s$ –step ahead prediction setting ( $S = 1$  refers to examples in earlier sections). Features  $X_t := [Y_{t-1}, \dots, Y_{t-w}]$  are auto-regressive with a pre-specified window  $w \geq 1$ . At prediction time  $t$ , we need to construct  $S$  prediction intervals at once for

Table 2: Marginal coverage and width by all methods on three real time series. The target coverage is 0.9, and entries in the bracket indicate standard deviation over three independent trials. It is clear that **SPCI** outperforms competitors with a much narrower interval width and does not have interval validity.

	Wind coverage	Wind width	Electric coverage	Electric width	Solar coverage	Solar width
SPCI	0.95 (0.00e+00)	2.65 (1.60e-02)	0.93 (4.79e-03)	0.22 (1.68e-03)	0.91 (1.12e-02)	47.61 (1.33e+00)
EnbPI	0.93 (6.20e-03)	6.38 (3.01e-02)	0.91 (6.84e-04)	0.32 (9.11e-04)	0.88 (4.25e-03)	48.95 (3.38e+00)
AdaptiveCI	0.95 (5.37e-03)	9.34 (3.56e-02)	0.95 (1.81e-03)	0.51 (7.25e-03)	0.96 (1.39e-02)	56.34 (1.15e+00)
NEXCP	0.96 (8.21e-03)	6.68 (7.73e-02)	0.90 (2.05e-03)	0.45 (2.16e-03)	0.90 (7.73e-03)	102.80 (5.25e+00)

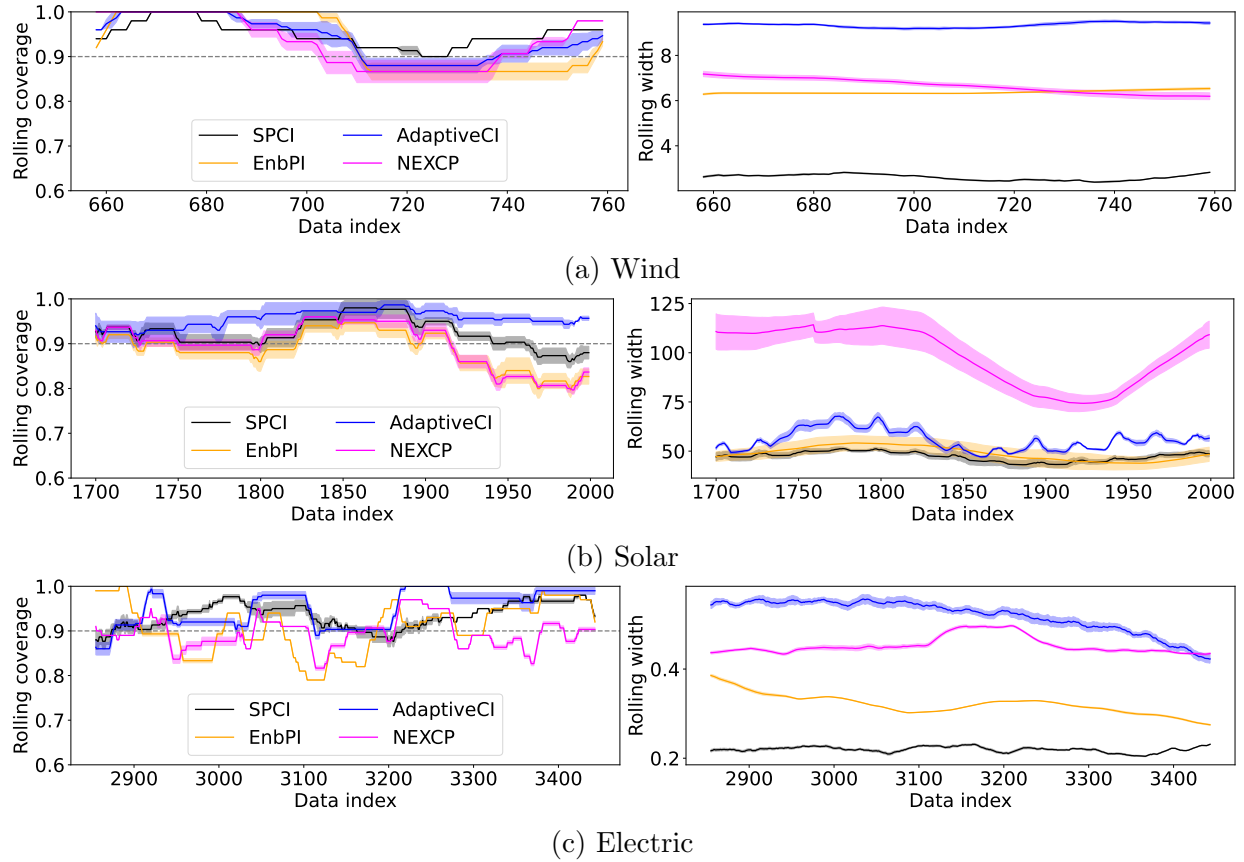


Figure 5: Rolling coverage and interval width over three real time series by different methods. It is clear that SPCI in black not only yields valid rolling coverage but also consistently yields the narrowest prediction intervals. Furthermore, the variance of SPCI results over trials is also small, as shown by the shaded regions over coverage and width results.

time indices  $t, \dots, t + S - 1$ . In particular, responses  $Y_t, \dots, Y_{t+S-1}$  (and thus features  $X_{t+1}, \dots, X_{t+S}$ ) are not available until we predict for indices  $t + S, \dots, t + 2S - 1$ .

*Multi-step SPCI algorithm.* Note that constructing multi-step ahead prediction intervals using SPCI involves estimating the *joint* distribution of  $\hat{\epsilon}_{t+1}, \dots, \hat{\epsilon}_{t+S}$  every  $S$  test indices. Doing so can be highly challenging. Instead, we take a simplified “divide-and-conquer” approach. For concreteness, we train LOO point predictors based on EnbPI [Xu and Xie, 2021], making more accurate point predictions than split conformal methods in practice. First, we train  $S$  sets of LOO predictors for estimating the value of  $\hat{Y}_{t+j}, j = 0, \dots, S - 1$ . This is implemented by fitting  $B$  bootstrap models on each lagged data  $\{(X_t, Y_{t+s})\}_{t=1}^{T-s+1}, s = 1, \dots, S$ . Then, we compute residuals only at  $t = 1 + kS : kS \leq T - 1$ . We do so because on test data, new feature  $X_t$  and output  $Y_t$  are revealed only in every  $S$  step. Lastly, we fit QRF  $S$  times using past residuals with lags to obtain  $s$  prediction

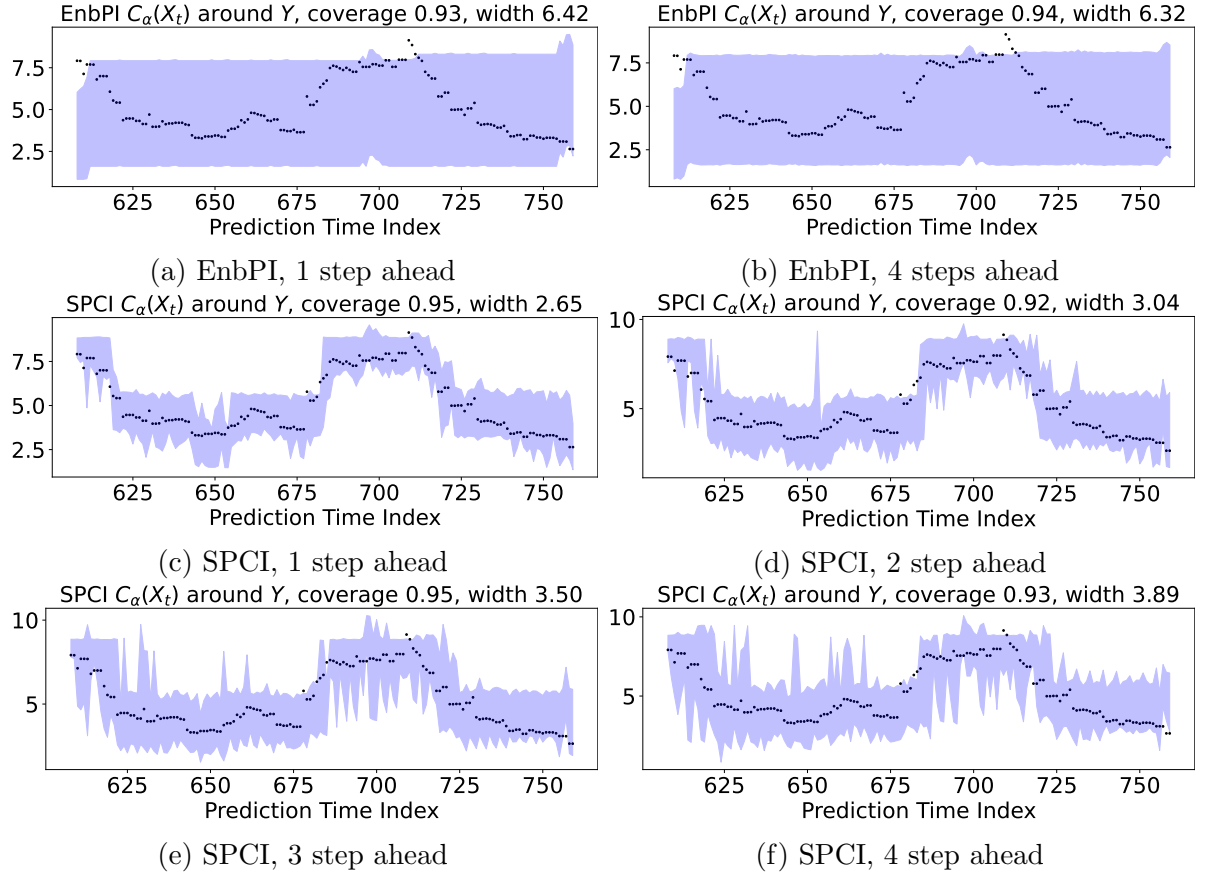


Figure 6: Multi-step ahead prediction interval construction by SPCI and EnbPI on wind speed data. Compared to EnbPI results in subfigures (a) and (b), SPCI intervals are much narrower and more adaptive—SPCI intervals follow the trajectory of the original time-series whereas EnbPI are overly conservative. In addition, SPCI interval widths increase as the predictive horizon increases, reflecting the existence of more uncertainty in point predictions further into the future.

intervals at once. Details appear in Algorithm 3.

We briefly compare and contrast Algorithm 1 (SPCI) and 3 (multi-step ahead SPCI) when LOO point predictors are trained. Computationally, we need to refit  $S - 1$  more sets of LOO predictors in multi-step ahead SPCI for point prediction. On the other hand, both algorithms fit the same number of QRF regressors for constructing prediction intervals. In practice, multi-step SPCI is expected to yield wider intervals as  $S$  increases because there is greater uncertainty when fitting the baseline regression or QRF on lagged data. A simple example is the  $AR(1)$  process where  $x_t = ax_{t-1} + \epsilon_t$ ,  $\epsilon_t \stackrel{i.i.d.}{\sim} N(0, 1)$ . Using the present feature  $x_{t-1}$ , we have  $x_{t+S} = a^{S+1}x_{t-1} + \sum_{i=1}^S a^{i-1}\epsilon_{t+i}$ , whereby the error distribution  $a^{i-1}\epsilon_{t+i} \sim N(0, \sum_{i=1}^S a^{2(i-1)})$ , so width naturally increases.

---

**Algorithm 3** Multi-step SPCI (based on LOO prediction in EnbPI [Xu and Xie, 2021])

---

**Require:** Training data  $\{(X_t, Y_t)\}_{t=1}^T$ , significance level  $\alpha$ , number of bootstrap estimators  $B$ , aggregation function  $\phi$ , conditional quantile regression algorithm  $\mathcal{Q}$ , multi-step size  $S > 1$ .

**Ensure:** Prediction intervals  $\hat{C}_{t-1}(X_t), t > T$

- 1: **for**  $s = 1, \dots, S$  **do**  $\{\triangleright s\text{-step ahead model fitting}\}$
- 2:   Sample with replacement  $B$  index sets, each of size  $T - s + 1$ :  
 $\{S_b : S_b \subset \{1, \dots, T - s + 1\}\}_{b=1}^B$ .
- 3:   Train  $B$  corresponding bootstrap estimators  $\{\hat{f}^b\}_{b=1}^B$  on data  $\{(X_t, Y_{t+s-1}) : t \in S_b\}$ .  
 $\{\triangleright \text{Leave-one-out aggregation}\}$
- 4:   Initialize  $\hat{\epsilon} = []$
- 5:   **for**  $t = 1, 1 + S, \dots, 1 + kS$  such that  $kS \leq T - 1$  **do**
- 6:      $\hat{f}_t^s(X_t) = \phi(\{\hat{f}^b(X_t), t \notin S_b\}_{b=1}^B)$
- 7:      $\hat{\epsilon}.append(Y_{t+s-1} - \hat{f}_t^s(X_t))$
- 8:   **end for**
- 9: **end for**
- 10: **for**  $t > T$  **do**  $\{\triangleright \text{Interval construction}\}$
- 11:   Compute  $s := \text{mod}(t - T, S + 1)$  and  $t' := t - s$   
 $\{\triangleright t'$  denotes the most recent index where residual  $\hat{\epsilon}_{t'}$  and feature  $X_{t'+1}$  are available. $\}$
- 12:   **if**  $s = 1$  **then**  $\{\triangleright \text{Re-fit quantile regressors and update residuals}\}$
- 13:     Re-fit  $S$  quantile estimators  $\{\hat{Q}_t(\cdot; s)\}_{s=1}^S$  with  $\{(\hat{\epsilon}_j^w, \hat{\epsilon}_{j+s-1})\}_{j=t-T+w}^{t-1-(S-1)}$ .
- 14:      $\hat{\epsilon}.pop(1)$  for  $S$  times and  $\hat{\epsilon}.append(Y_t - \hat{Y}_t)$ .  $\{\triangleright \text{Skip this step at } t = T + 1.\}$
- 15:   **end if**
- 16:   Compute  $\hat{\beta} = \arg \min_{\beta \in [0, \alpha]} (\hat{Q}_t(1 - \alpha + \beta; s) - \hat{Q}_t(\beta; s))$  using  $\hat{\epsilon}_{t'}^w$ .
- 17:    $\hat{C}_{t-1}(X_t) = [\hat{Y}_t + w_{\text{left}}(t), \hat{Y}_t + w_{\text{right}}(t)]$ , where  
 $\hat{Y}_t = \phi(\{\hat{f}_j^s(X_{t'+1})\}_{j=1}^{T/S})$ ,  $w_{\text{left}}(t) = \hat{Q}_t(\hat{\beta}; s)$ ,  $w_{\text{right}}(t) = \hat{Q}_t(1 - \alpha + \hat{\beta}; s)$  .
- 18: **end for**

---

*Result.* Figure 6 compares SPCI with EnbPI on the wind dataset in terms of multi-step ahead coverage and width—EnbPI supports multi-step ahead prediction in the algorithm, although each batch of  $S$ -step ahead intervals have the same width by construction. We note that (1) EnbPI intervals are too wide and non-adaptive, as 4-step ahead intervals may even be narrower than 1-step ahead ones. (2) In contrast, SPCI intervals closely follow the trajectory of actual data and are more adaptive:  $S$ -step ahead intervals with larger  $S$  yield wider average widths, aligning with our expectations.

## 7 Conclusions

In this work, we propose **SPCI**, a general framework for constructing prediction intervals for time series. Similar to existing conformal prediction methods, **SPCI** is model-free and distribution-free, making it applicable to any time series with arbitrary predictive models. Unlike existing CP methods, **SPCI** fits quantile regression models on *non-conformity scores* to utilize temporal dependency among non-conformity scores to achieve more adaptive confidence intervals and better coverage. Theoretical analyses verify the asymptotic valid conditional coverage by **SPCI**. Experimental results consistently show improved performance by **SPCI** over existing sequential conformal prediction methods.

These questions currently remain open. First, we wish to quantify uncertainty in multi-variate time-series prediction. Naive use of **SPCI** builds separate prediction intervals for each uni-variate time series. However, doing so ignores the joint distribution among non-conformity scores of each uni-variate time series. The resulting prediction region (i.e., a hypercube) would thus be sub-optimal. Second, we want to refine the multi-step ahead **SPCI** in Algorithm 3 to better capture the joint distribution of multi-step predictions. Providing similar performance guarantees is also an important research direction in this case.

## Acknowledgement

This work is partially supported by an NSF CAREER CCF-1650913, and NSF DMS-2134037, CMMI-2015787, DMS-1938106, and DMS-1830210.

## References

Anastasios N Angelopoulos and Stephen Bates. A gentle introduction to conformal prediction and distribution-free uncertainty quantification. *arXiv preprint arXiv:2107.07511*, 2021.

Anastasios Nikolas Angelopoulos, Stephen Bates, Michael Jordan, and Jitendra Malik. Uncertainty sets for image classifiers using conformal prediction. In *International Conference on Learning Representations*, 2021. URL [https://openreview.net/forum?id=eNdiU\\_DbM9](https://openreview.net/forum?id=eNdiU_DbM9).

Rina Foygel Barber, Emmanuel J Candes, Aaditya Ramdas, and Ryan J Tibshirani. Conformal prediction beyond exchangeability. *arXiv preprint arXiv:2202.13415*, 2022.

Gérard Biau and Benoît Patra. Sequential quantile prediction of time series. *IEEE Transactions on Information Theory*, 57(3):1664–1674, 2011.

Leo Breiman. Random forests. *Machine learning*, 45(1):5–32, 2001.

Peter J Brockwell, Richard A Davis, and Stephen E Fienberg. Time series: theory and methods: theory and methods. *Springer Science & Business Media*, 1991.

Zongwu Cai. Regression quantiles for time series. *Econometric theory*, 18(1):169–192, 2002.

Jaquelin Cochran, Paul Denholm, Bethany Speer, and Mackay Miller. Grid integration and the carrying capacity of the us grid to incorporate variable renewable energy. Technical report, National Renewable Energy Lab.(NREL), Golden, CO (United States), 2015.

William J. Cody and Henry C. Thacher. Chebyshev approximations for the exponential integral. *Mathematics of Computation*, 23:289–303, 1969.

Francisco Díaz-González, Andreas Sumper, Oriol Gomis-Bellmunt, and Roberto Villafáfila-Robles. A review of energy storage technologies for wind power applications. *Renewable and sustainable energy reviews*, 16(4):2154–2171, 2012.

Robert F. Engle. Autoregressive conditional heteroscedasticity with estimates of the variance of united kingdom inflation. *Econometrica*, 50:987–1007, 1982.

Rina Foygel Barber, Emmanuel J Candes, Aaditya Ramdas, and Ryan J Tibshirani. The limits of distribution-free conditional predictive inference. *Information and Inference: A Journal of the IMA*, 10(2):455–482, 2021.

Isaac Gibbs and Emmanuel Candes. Adaptive conformal inference under distribution shift. *Advances in Neural Information Processing Systems*, 34:1660–1672, 2021.

Chirag Gupta, Arun K Kuchibhotla, and Aaditya Ramdas. Nested conformal prediction and quantile out-of-bag ensemble methods. *Pattern Recognition*, page 108496, 2021.

M. Harries, University of New South Wales. School of Computer Science, and Engineering. *Splice-2 Comparative Evaluation: Electricity Pricing*. PANDORA electronic collection. University of New South Wales, School of Computer Science and Engineering, 1999.

Stéphane Lathuilière, Pablo Mesejo, Xavier Alameda-Pineda, and Radu Horaud. A comprehensive analysis of deep regression. *IEEE transactions on pattern analysis and machine intelligence*, 2019.

Nicolai Meinshausen. Quantile regression forests. *J. Mach. Learn. Res.*, 7:983–999, 2006.

H. Papadopoulos, V. Vovk, and A. Gammerman. Conformal prediction with neural networks. In *19th IEEE International Conference on Tools with Artificial Intelligence(ICTAI 2007)*, volume 2, pages 388–395, 2007.

C. J. Ridder-Rowe. *Journal of the Royal Statistical Society. Series A (General)*, 131(2):230–231, 1968. ISSN 00359238. URL <http://www.jstor.org/stable/2343845>.

Yaniv Romano, Evan Patterson, and Emmanuel Candes. Conformalized quantile regression. In *Advances in Neural Information Processing Systems*, pages 3543–3553, 2019.

Yaniv Romano, Matteo Sesia, and Emmanuel Candes. Classification with valid and adaptive coverage. *Advances in Neural Information Processing Systems*, 33:3581–3591, 2020.

Halsey Lawrence Royden and Patrick Fitzpatrick. *Real analysis*, volume 32. Macmillan New York, 1988.

Glenn Shafer and Vladimir Vovk. A tutorial on conformal prediction. *Journal of Machine Learning Research*, 9(Mar):371–421, 2008.

Aad W Van der Vaart. *Asymptotic statistics*, volume 3. Cambridge university press, 2000.

Zhijie Xiao. Time series quantile regressions. In *Handbook of statistics*, volume 30, pages 213–257. Elsevier, 2012.

Chen Xu and Yao Xie. Conformal anomaly detection on spatio-temporal observations with missing data. In *ICML 2021 Workshop on Distribution-free Uncertainty Quantification*, 2021.

Margaux Zaffran, Aymeric Dieuleveut, Olivier F’eron, Yannig Goude, and Julie Josse. Adaptive conformal predictions for time series. In *ICML*, 2022.

Gianluca Zeni, Matteo Fontana, and Simone Vantini. Conformal prediction: a unified review of theory and new challenges. *arXiv preprint arXiv:2005.07972*, 2020.

Zhou Zhou and Wei Biao Wu. Local linear quantile estimation for nonstationary time series. *The Annals of Statistics*, 37(5B):2696–2729, 2009.

Shixiang Zhu, Hanyu Zhang, Yao Xie, and Pascal Van Hentenryck. Multi-resolution spatio-temporal prediction with application to wind power generation. In *2022 INFORMS Workshop on Data Science*, 2021.

## A Proof

*Proof of Lemma 1.* First, by [Ridler-Rowe, 1968, Theorem 1, p.127-128], we know that (17) implies

$$\sup_{y \in \mathbb{R}} |\hat{F}(y|x) - F(y|x)| \rightarrow 0 \text{ in probability.} \quad (23)$$

Recall that  $Q(p)$  is unique. Thus, for any  $x$ , there exists  $\epsilon = \epsilon(x) > 0$  such that

$$\delta = \delta(\epsilon) := \min\{p - F(Q(p) - \epsilon|x), F(Q(p) + \epsilon|x) - p\} > 0.$$

Namely, there exists a small perturbation of  $Q(p)$  whereby the change in the value of the distribution function is at least positive. Thus, we have that

$$\begin{aligned}\mathbb{P}(|\widehat{Q}(p) - Q(p)| > \epsilon) &\stackrel{(i)}{=} \mathbb{P}(|F(\widehat{Q}(p)|x) - p| > \delta) \\ &= \mathbb{P}(|F(\widehat{Q}(p)|x) - \hat{F}(\widehat{Q}(p)|x)| > \delta) \\ &\leq \mathbb{P}(\sup_{y \in \mathbb{R}} |F(y|x) - \hat{F}(y|x)| > \delta).\end{aligned}$$

Note that (i) holds because the event  $|\widehat{Q}(p) - Q(p)| > \epsilon$  means that  $\widehat{Q}(p)$  is at least  $\epsilon$  far away from  $Q(p)$ . By monotonicity of the distribution function  $F$ , this event implies the occurrence of the event  $|F(\widehat{Q}(p)|x) - p| > \delta$ .

Now, (23) implies the convergence of estimated quantile values, hence finishing the proof.  $\square$

To prove Proposition 2, we need the following assumptions.

**Assumption 1.** Define  $U_t := F(Y_t|X = X_t)$  as the quantile of observations  $Y_t$  conditioning on the feature  $X_t$ , where  $U_t \sim \text{Unif}[0, 1]$ . For a  $x \in \mathcal{B} := \text{Supp}(\{X_t\}_{t \geq 1})$ , define the scalar  $z[x] := F(y|X = x)$ . Given

$$g(i, j, x_1, x_2) := \text{Cov}(\mathbb{1}(U_i \leq z[x_1]), \mathbb{1}(U_j \leq z[x_2])),$$

we require that for any pair of  $x_1, x_2 \in \mathcal{B}$ ,

$$g(i, j, x_1, x_2) = g(|i - j|) \text{ for } i \neq j \quad (24)$$

In addition,  $g(k)$  in (24) needs to satisfy

$$\lim_{T \rightarrow \infty} \left[ \int_1^T \int_1^x g(u) du dx \right] / T^2 \rightarrow 0. \quad (25)$$

In other words, Assumption 1 assumes that the covariance of the indicator random variables, regardless of the value of  $z[x]$ , only depends on the difference in index. In addition, (25) restricts the order of growth of the function  $g(k)$ ,  $k \geq 1$  in (24). We note that (24) appears widely in the *weak or wide-sense stationary* processes, where the difference is that we do not require constant mean values of the indicator variables. In fact, constant mean is impossible, as  $\mathbb{E}[\mathbb{1}(U_t \leq z[x])] = z[x]$ , whose value changes depending on  $x$  and  $y$ .

Below are examples of  $g(k)$  in (24) for which (25) holds. We can also characterize the decay rate of (25).

**Example 1** (Finite memory). For some cutoff index  $s \in \mathbb{Z}$  and constants  $\{c_1, \dots, c_s\}$ ,

$$g(k) = \begin{cases} c_k & k \leq s \\ 0 & k > s \end{cases}$$

Showing  $g(k)$  in Example 1 satisfies (25) is trivial, with decay rate  $O(1/T^2)$ . Meanwhile, the example holds for stochastic processes with finite memory. That is,  $\text{Cov}(U_t, U_j) = 0$  if  $|i - j| > s$  for  $U_i, U_j$  defined in Assumption 1.

**Example 2** (Linear decay). *For every  $k \geq 1$ ,  $g(k) = \frac{1}{k^p}, p \geq 1$ .*

Example 2 is weaker than Example 1, where we see that

$$\begin{aligned} \int_1^T \int_1^x g(u) du dx &= \int_1^T \int_1^x 1/u du dx \\ &= \int_1^T \log(x) dx = T(\log T - 1). \end{aligned}$$

Thus,  $T^{-2} \int_1^T \int_1^x g(u) du dx = \frac{T(\log T - 1)}{T^2} = O(\log(T)/T)$ . Hence, (25) is proven for Example 2.

**Example 3** (Logarithmic decay). *For every  $k \geq 1$ ,  $g(k) = \left[ \frac{1}{\log(k+1)} \right]^p, p \geq 1$ .*

Example 3 is weaker than the above two examples as it imposes a weaker decay order on the covariance. Lemma 2 presents the proof of (25) for this example, which decays at the order of  $O(\frac{1}{2 \log T})$ . In general, we wish to show (25) in this example when  $p \in (0, 1)$ . However, doing so is difficult as the analysis of the integral  $\int_1^T \int_1^x [\frac{1}{\log(u+1)}]^p du dx$  is complicated. Furthermore, note that  $\log(u+1)^p \rightarrow 1$  as  $p \rightarrow 0$ , so this integral tends to  $T^2/2$ , whereby (25) cannot be obtained for small enough  $p$ .

**Assumption 2.** *The weights  $w_t(x)$  in (15) satisfies that for all  $x \in \mathbb{B}$ ,  $w_t(x) = O(1/T)$ .*

Assumption 2 imposes the condition on the decay order of each weights. Note that by the definition of  $w_t(x)$  in (15) and [Meinshausen, 2006, Assumption 2], we know that  $w_t(x) = o(1)$ . Assumption 2 thus assumes an exact order of decay of the weights.

**Assumption 3.** *The true conditional distribution function is Lipschitz continuous with parameter  $L$ . That is, for all  $x, x'$  in the support of the random variable  $X$ .*

$$\sup_y |F(y|X=x) - F(y|X=x')| \leq L \|x - x'\|_1.$$

**Assumption 4.** *For every  $x$  in the support of  $X$ , the conditional distribution function  $F(y|X=x)$  is continuous and strictly monotonically increasing in  $y$ .*

We remark that Assumption 3 and 4 are identical to [Meinshausen, 2006, Assumption 4 and 5], respectively.

We also need a technical lemma before proving this Proposition.

**Lemma 2.** For  $p \geq 1$ , we have

$$\lim_{T \rightarrow \infty} \left[ \int_1^T \int_2^x \frac{1}{\log(u)^p} dudx \right] / n^2 = O\left(\frac{1}{2 \log T}\right).$$

*Proof of Lemma 2.* First, consider the case where  $p = 1$ . Define  $li(x)$  as the anti-derivative of  $1/\log(x)$ . To find the growth order of  $li(x)$ , we note that  $li(x) = Ei(\log x)$ , where  $Ei(x)$  standards for the *exponential integral* with the form  $Ei(x) = \int_{-\infty}^x \frac{e^t}{t} dt$ . This can be shown via the change of variable  $\log(u) = t$ . Note that we have the following asymptotic expansion for  $Ei(x)$  [Cody and Thacher, 1969]:

$$\begin{aligned} Ei(x) &= \frac{\exp(x)}{x} \left(1 + \frac{1}{x} + \frac{2}{x^2} + \frac{6}{x^3} + \dots\right) \\ &= \frac{\exp(x)}{x} (1 + O(1/x)) \text{ when } x > 1. \end{aligned}$$

Thus,  $Ei(\log x) = \frac{x}{\log x} (1 + O(1/\log x)) \approx \frac{x}{\log x}$  for large  $x$ .

As a result, dropping the constants and small order terms yield

$$\begin{aligned} \int_1^T \int_2^x \frac{1}{\log(u)} dudx &= \int_1^T Ei(\log x) dx \\ &= \int_1^T \frac{x}{\log x} dx \\ &= Ei(2 \log T) \end{aligned}$$

Hence, we have

$$\begin{aligned} \lim_{T \rightarrow \infty} \left[ \int_1^T \int_2^x \frac{1}{\log(u)} dudx \right] / n^2 &= \lim_{T \rightarrow \infty} Ei(2 \log T) / T^2 \\ &= O\left(\frac{1}{2 \log T}\right). \end{aligned}$$

Lastly, when  $p > 1$ ,  $\frac{1}{\log u} > [\frac{1}{\log u}]^p$  uniformly for all  $u > 1$ . Hence, we have

$$\lim_{T \rightarrow \infty} \left[ \int_1^T \int_2^x \frac{1}{\log(u)^p} dudx \right] / T^2 < \lim_{T \rightarrow \infty} \left[ \int_1^T \int_2^x \frac{1}{\log(u)} dudx \right] / T^2,$$

where the latter limit decays at order  $O(\frac{1}{2 \log T})$  as shown above.  $\square$

*Proof of Proposition 2.* The proof is motivated by the analyses in [Meinshausen, 2006]. In essence, we analyze the point-wise difference between the estimate  $\hat{F}(y|x)$  in (16) and the true value  $F(y|x)$ . The difference can then be broken into two terms. Both terms can be bounded by Chebyshev inequalities, leading to convergence to zero.

First, for each observation  $t = 1, \dots, T$ , denote  $U_t := F(Y_t|X = X_t)$  as the quantile of the  $t$ -th observation. Note that  $U_t \sim \text{Unif}[0, 1]$  by the property of the distribution function.

Now, by the form of the estimator  $\hat{F}(y|x)$  in (16), we break it into two parts:

$$\begin{aligned}\hat{F}(y|x) &= \sum_{t=1}^T w_t(x) \mathbb{1}(Y_t \leq y) \\ &\stackrel{(i)}{=} \sum_{t=1}^T w_t(x) \mathbb{1}(U_t \leq F(y|X_t)) \\ &= \sum_{t=1}^T w_t(x) \mathbb{1}(U_t \leq F(y|x)) + \sum_{t=1}^T w_t(x) (\mathbb{1}(U_t \leq F(y|X_t)) - \mathbb{1}(U_t \leq F(y|x))).\end{aligned}$$

The equivalence (i) holds because the event  $\{Y_t \leq y\}$  is identical to the event  $\{U_t \leq F(y|x = X_t)\}$  under Assumption 4. Thus, we have that

$$\begin{aligned}|\hat{F}(y|x) - F(y|x)| &\leq \underbrace{\left| \sum_{t=1}^T w_t(x) \mathbb{1}(U_t \leq F(y|x)) - F(y|x) \right|}_{(a)} + \\ &\quad \underbrace{\left| \sum_{t=1}^T w_t(x) (\mathbb{1}(U_t \leq F(y|X_t)) - \mathbb{1}(U_t \leq F(y|x))) \right|}_{(b)}.\end{aligned}$$

1) *Bound of term (a).* The first term can be bounded using Chebyshev inequality. Let  $z := F(y|x)$ . Define  $U' := \sum_{t=1}^T w_t(x) \mathbb{1}(U_t \leq z)$ . By the linearity of expectation taken over  $U_t$ , we have

$$\begin{aligned}\mathbb{E}[U'] &= \sum_{t=1}^T w_t(x) \mathbb{E}[\mathbb{1}(U_t \leq z)] \\ &= \left[ \sum_{t=1}^T w_t(x) \right] z \stackrel{(i)}{=} z,\end{aligned}$$

where (i) holds under the definition of  $w_t(x)$  in (15), which satisfies  $\sum_{t=1}^T w_t(x) = 1$  as remarked earlier. Now, for any  $\epsilon > 0$ ,

$$\begin{aligned}&\mathbb{P} \left( \left| \sum_{t=1}^T w_t(x) \mathbb{1}(U_t \leq F(y|x)) - F(y|x) \right| \geq \epsilon \right) \\ &= \mathbb{P}(|U' - z| \geq \epsilon) \leq \text{Var}(U')/\epsilon^2.\end{aligned}$$

Note that

$$\begin{aligned}
\text{Var}(U') &= \text{Var}\left(\sum_{t=1}^T w_t(x) \mathbb{1}(U_t \leq z)\right) \\
&= \underbrace{\sum_{t=1}^T w_t(x)^2 \text{Var}(\mathbb{1}(U_t \leq z))}_{(i)} + \underbrace{\sum_{i \neq j} w_i(x) w_j(x) \text{Cov}(\mathbb{1}(U_i \leq z), \mathbb{1}(U_j \leq z))}_{(ii)}. \quad (26)
\end{aligned}$$

We need to show that (i) and (ii) in (26) both converge to zero. To show the convergence of (i), we have  $w_t(x) = O(1/T)$  by Assumption 2 and note that  $\text{Var}(\mathbb{1}(U_t \leq z)) = \mathbb{E}(\mathbb{1}(U_t \leq z)^2) - E(\mathbb{1}(U_t \leq z))^2 = z - z^2$ . Hence,  $\text{Var}(\mathbb{1}(U_t \leq z)) < 1$  and we have  $\sum_{t=1}^T w_t(x)^2 \text{Var}(\mathbb{1}(U_t \leq z)) < \sum_{t=1}^T w_t(x)^2 = O(1/T)$ .

To show the convergence of (ii), we have by Assumption 1 that

$$\begin{aligned}
\sum_{i \neq j} w_i(x) w_j(x) \text{Cov}(\mathbb{1}(U_i \leq z), \mathbb{1}(U_j \leq z)) &= \sum_{k=1}^{T-1} \frac{T-k}{T^2} g(k) \\
&\leq \int_1^T \frac{T-k}{T^2} g(k) dk \\
&= T^{-1} \int_1^T g(k) dk - T^{-2} \int_1^T k g(k) dk \\
&= T^{-1} [G(T) - G(1)] - T^{-2} \int_1^T k g(k) dk,
\end{aligned}$$

where  $G(x) := \int_1^x g(k) dk$  is the anti-derivative of  $g$ . Using integration by part with  $u = k, dv = g(k) dk$ , we have

$$\int_1^T k g(k) dk = T G(T) - G(1) - \int_1^T G(x) dx.$$

Thus, dropping constants and small order terms yield

$$\sum_{i \neq j} w_i(x) w_j(x) \text{Cov}(\mathbb{1}(U_i \leq z), \mathbb{1}(U_j \leq z)) \leq \left[ \int_1^T \left[ \int_1^x g(k) dk \right] dx \right] / T^2.$$

By (25) in Assumption 1, we thus have the desired convergence result.

2) *Bound of term (b).* Define  $W := \sum_{t=1}^T w_t(x) \mathbb{1}(U_t \leq F(y|X_t))$ . Note that  $\mathbb{E}(W) = \sum_{t=1}^T w_t(x) F(y|X_t)$ . We have for any  $\epsilon > 0$ ,

$$\begin{aligned}
&\mathbb{P}(|W - \mathbb{E}(W)| > \epsilon) \\
&\leq \text{Var}(W) / \epsilon^2 \\
&= (\epsilon)^{-2} \left[ \sum_{t=1}^T w_t(x)^2 \text{Var}(\mathbb{1}(U_t \leq F(y|X_t))) + \sum_{i \neq j} w_i(x) w_j(x) \text{Cov}(\mathbb{1}(U_i \leq F(y|X_i)), \mathbb{1}(U_j \leq F(y|X_j))) \right].
\end{aligned}$$

By the same argument for bounding term (a) above, we have that  $W \xrightarrow{p} \mathbb{E}[W]$  as sample size  $T \rightarrow \infty$ .

As a result, we have

$$\left| \sum_{t=1}^T w_t(x)(\mathbb{1}(U_t \leq F(y|X_t)) - \mathbb{1}(U_t \leq F(y|x))) \right| \xrightarrow{p} \left| \sum_{t=1}^T w_t(x)(F(y|X_t) - F(y|x)) \right|.$$

By Assumption 3, we have

$$\left| \sum_{t=1}^T w_t(x)(F(y|X_t) - F(y|x)) \right| \leq \sum_{t=1}^T w_t(x)L\|X_t - x\|_1.$$

The rest of proof follows due to [Meinshausen, 2006, Lemma 2], which shows that

$$\sum_{t=1}^T w_t(x)\|X_t - x\|_1 = o_p(1).$$

□

*Proof of Theorem 1.* Under SPCI interval construction in (10), the equivalence in (6) implies that

$$\mathbb{P}(Y_t \in \hat{C}_{t-1}(X_t)|X_t) = F(\hat{Q}_t(1 - \alpha + \hat{\beta})|\mathcal{E}_t^w) - F(\hat{Q}_t(\hat{\beta})|\mathcal{E}_t^w),$$

where  $\hat{Q}_t(p), p \in [0, 1]$  is the estimated  $p$ -th quantile of  $\hat{\epsilon}_t$ ,  $F(w|\mathcal{E}_t^w)$  is the unknown distribution function of  $\hat{\epsilon}_t$ , and  $\hat{\beta}$  minimizes interval width per the procedure in Algorithm 1.

To finish the proof, by Proposition 2, we know that the conditional distribution estimator  $\hat{F}(w|\mathcal{E}_t^w)$  using QRF converges point-wise to the true  $F(w|\mathcal{E}_t^w)$  as the sample size (hence the number of residuals) approaches infinity. By Lemma 1, we thus know that  $\hat{Q}_t(p) \rightarrow Q_t(p)$  in probability for all  $p \in [0, 1]$ .

We can thus use the continuous mapping theorem [Van der Vaart, 2000, Theorem 2.3] to finish the proof: by Assumption 3, the set of discontinuity points of the true conditional distribution  $F$  has measure zero. Thus, as samples size  $T \rightarrow \infty$ , in probability,

$$\begin{aligned} & F(\hat{Q}_t(1 - \alpha + \hat{\beta})|\mathcal{E}_t^w) - F(\hat{Q}_t(\hat{\beta})|\mathcal{E}_t^w) \\ & \rightarrow F(Q_t(1 - \alpha + \hat{\beta})|\mathcal{E}_t^w) - F(Q_t(\hat{\beta})|\mathcal{E}_t^w) = 1 - \alpha. \end{aligned}$$

□